Journal of
Materials Chemistry C

Accepted Manuscript

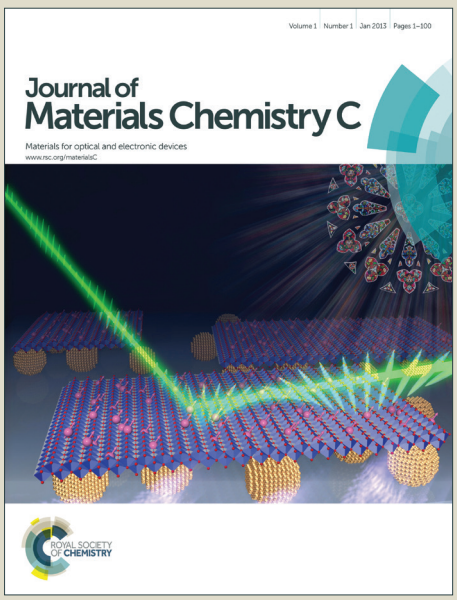

ROYAL SOCIETY OF CHEMISTRY

www.rsc.org/materialsC

Graphical Abstract

Water soluble ribbon-like g-C_3N_4 and various special assemblies were obtained from dicyandiamide using NaCl crystals as a hard template.

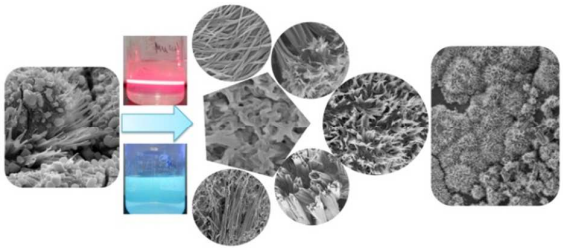

Cite this: DOI: 10.1039/c0xx00000x

www.rsc.org/xxxxxx

ARTICLE TYPE

Water-soluble ribbon-like graphitic carbon nitride (g-C_3N_4): green synthesis, self-assembly and unique optical properties

Bo Yuan, Zengyong Chu*, Gongyi Li, Zhenhua Jiang, Tianjiao Hu, Qinghua Wang, and Chunhua Wang

Received (in XXX, XXX) Xth XXXXXXXXX 20XX, Accepted Xth XXXXXXXXX 20XX
DOI: 10.1039/b000000x

Ribbon-like g-C_3N_4 was obtained from dicyandiamide using NaCl crystals as the template. The texture modification leads to an increased band gap to 3.0 eV with much stronger photoluminescence intensity. Hydrogen bonding offers them exceptional stable dispersion in water. Upon adding different alcohols, various special assemblies could precipitate from the dispersion.

During the past several years, much attention has been paid to a non-metal semiconductor, graphitic carbon nitride (g-C_3N_4).[1-6] g-C_3N_4 is the most stable allotrope in carbon nitride materials and has a small direct band gap of ~2.7eV, exhibiting excellent sunlight harvesting capability. It is a good visible-light photocatalyst for the degradation of pollutions,[7-8] water splitting,[9] organic synthesis[10] and oxygen reduction.[11] Under the excitation of light or electricity, g-C_3N_4 emits high fluorescence[12] and can be used as an effective photosensor for Cu^{2+},[13-14] Fe^{3+} [15] and rutin.[16] Moreover, g-C_3N_4 is robust and non-volatile under light irradiation, even in acid or base solutions and up to 600℃, so g-C_3N_4 could be used as excellent photoelectronic and photoelectron chemical anti-corrosion materials.[17-19] In addition, g-C_3N_4 shows potential application as photosensitizes and drug nanocarriers for cancer imaging and therapy,[20-21] due to the excellent biocompatibility and non-toxicity. g-C_3N_4 is also a promising material for hydrogen storage based on the nitride pores. [22-23]

In general, g-C_3N_4 can be synthesized by the polymerization of molecular precursors, such as urea,[24] cyanamid,[25] dicyandiamide (DCDA),[26] melamine,[27] melamine hydrochloride[28] and melem.[29] However, g-C_3N_4 collected directly after self-condensation is a bulk material with very small surface area.[1-6] This limits its application in the above fields. Up to now, many new methods have been developed to modify the texture of g-C_3N_4, such as nanocasting using hard template or soft template,[30-33] chemical doping with sulfur or functional groups,[34-37] atomic sheet splitting via controlled oxidation or liquid exfoliation.[38-41] The chemical doping or the lower in dimension strongly modified the electronic properties of carbon nitride, and provided them with additional new functionality. For example, salts such as LiCl and LiCl/KCl have been used as melt solvents to make g-C_3N_4 with new polymeric structures;[37] ultrathin graphitic carbon nitride nanosheets have been shown to be a low-cost, green, and highly efficient electrocatalyst toward the reduction of hydrogen peroxide in addition to glucose biosensing.[39-41] But up to now, there is no report on the direct synthesis of g-C_3N_4 nanosheets or nanoribbons using salt crystals as the template.

In the present work, we report our attempt to modify the texture and morphology of g-C_3N_4 by a simple method using NaCl crystals as the hard and easy-to-remove template. The heat-treated DCDA/NaCl sample is an orange mixture, as shown in Fig. 1 (inset in a). Moldy microscale g-C_3N_4 could be observed growing directly from the interspaces or the surfaces of NaCl crystals (Fig. 1a). When the mixture was grounded, ultrasonic dispersed in water and centrifuged at 4000 rpm, a uniform dispersion could be obtained, which is stable even for more than half month (Fig. 1b-c). Sodium chloride was mostly removed through the dialysis bags (NaCl residual < 10 wt%, Fig. S1) and water was totally removed using the freeze-drying process. The final product, yield ~20wt%, looks white under sunlight and exhibits nanoscale ribbon-like morphology (Fig. 1d-f), seeming about 100~200nm wide and more than 1 μm long. They agglomerate promiscuously into a loose structure. It is the grinding, ultrasonic treatment and centrifuging that transforms the microscale mixture to the nanoscale product. HRTEM image (Fig. 1g) shows a typical lattice spacing of ~3.3nm, in agreement with the spacing of the (002) crystal planes of g-C_3N_4, 3.25nm.[1-6]

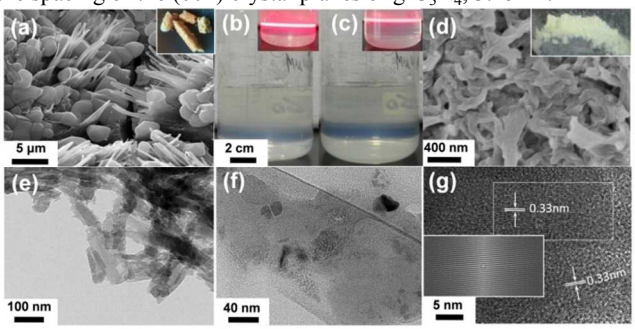

Figure 1. SEM images of (a) the heat treated DCDA/NaCl mixture and (d) the freeze-dried g-C_3N_4, optical images of (b-c) the water dispersion of NaCl-removed g-C_3N_4, TEM images of (e-g) the freeze-dried g-C_3N_4. NaCl is present in (a) and mostly removed in (b-g). The water dispersion was prepared and left for 0 day in (b) and 15 days in (c). The insets in (a and d) are the optical images of the corresponding samples; The inserts in (b and c) provide the Tyndall effect of the dispersion; the inset in (g) is the auto-correlation of the dashed square area.

Yellow bulk g-C_3N_4 was synthesized from pure DCDA for

comparison, which seems porous both at the micro and nano scales (Fig. S2).

Chemical structures of the products were characterized using Fourier transform infrared spectroscopy (FT-IR), X-ray diffraction (XRD), X-ray photoelectron spectroscopy (XPS) and thermogravimetric analysis (TGA), as shown in Fig. 2 and Fig. S3-4. For the bulk g-C_3N_4, several bands are found at 1200-1650 cm^{-1} (Fig. 2a), corresponding to the typical stretching modes of CN heterocyclic.[42] The peak at 810 cm^{-1} is indicative of the breathing mode of the triazine units.[37] The band at around 3100 cm^{-1} is caused by the residual N-H due to the incomplete polymerization of DCDA.[43] Besides these characteristic bands, there are also two obvious bands at around 2200 and 3450 cm^{-1} for the ribbon-like g-C_3N_4 (Fig. 2a). The strong band at 2200 cm^{-1} indicates the cyano group (−C≡N), which was regenerated by the catalytic pyrolysis of g-C_3N_4 above 550 ℃ (Fig. S3-4).

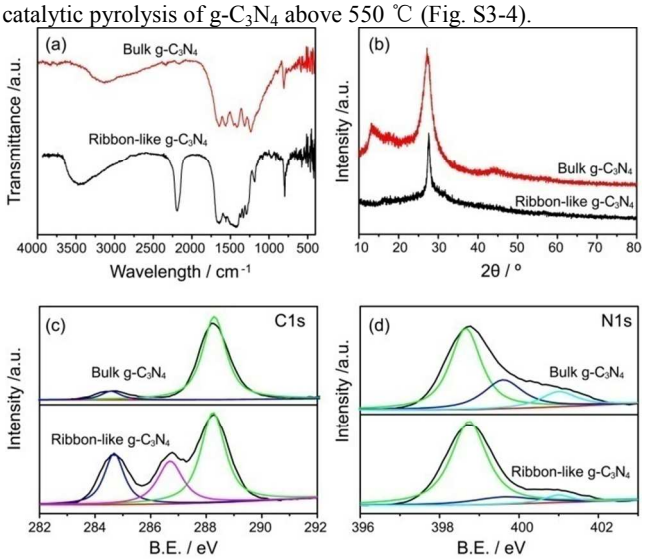

Figure 2. (a) FT-IR, (b) XRD, (c) XPS C1s, (d) XPS N1s of the bulk and the ribbon-like g-C_3N_4.

As shown in Fig. 2b, for the bulk g-C_3N_4, there are two peaks at around 13.2° and 27.4°, corresponding to the characteristic crystal faces of (100) and (002), respectively.[44] However, the peak at around 13.2° disappeared for the ribbon-like g-C_3N_4. Moreover, the main peak shifts slightly from 27.4° to 27.6°. This feature may be caused by the introduction of cyano groups, which can make interlayer stack denser by the formation of hydrogen bond between the g-C_3N_4 sheets.[45] As shown in Fig. 2c and d, the C1s and N1s peaks of the bulk and the ribbon-like g-C_3N_4 are almost identical, revealing that the network of g-C_3N_4 is mainly retained with the existence of NaCl.[14] In C1s spectra, both samples contain two common carbon species at 288.2 and 284.6 eV, corresponding to the C−N−C coordination and graphitic carbon.[22] For the ribbon-like g-C_3N_4, a new peak assigned to the C−CN group appeared at 286.7 eV. The binding energies of N1s spectra are determined to be 398.7, 399.6 and 401.0 eV (Fig. 2d). The main peak at 398.7 eV originates from the sp^2-bonded N involved in the triazine rings dominated in g-C_3N_4.[46] While the weak peaks at 399.6 and 401.0 eV indicate the presence of the tertiary nitrogen N−$(C)_3$ group and amino C−N−H.[47] Compared with the bulk g-C_3N_4, the latter two peaks of the ribbon-like g-C_3N_4 become weaker, indicating its much smaller sizes.

Diffuse reflectance spectroscopy (DRS), and photoluminescence (PL) were performed to characterize the optical properties, as shown in Fig. 3. The bulk g-C_3N_4 is yellow while the ribbon-like g-C_3N_4 is white under solar light. So the absorption edge of the ribbon-like g-C_3N_4 have a big blue shift, indicating an increased band gap from ~2.7 eV to ~3.0 eV. The lower in dimension generally increases the band gaps of g-C_3N_4 to some extent.[30-41] But, the incorporation of some Na^+ ions in the nitride pores and the introduction of some cyano groups may play the major role in increasing the band gaps.[37] Under 365nm UV light irradiation, the bulk g-C_3N_4 emits yellow light at around 510nm, while the ribbon-like g-C_3N_4 emits blue light at around 440nm, which is much stronger and very bright to naked eyes, even if in a water solution state.

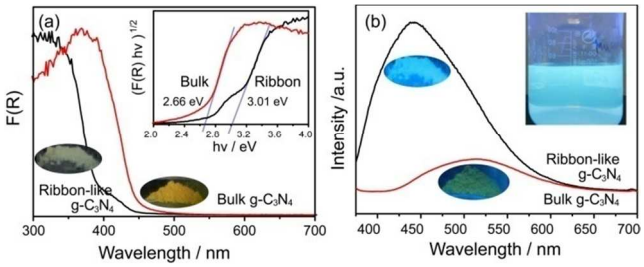

Figure 3. (a) DRS and (b) PL spectra of the bulk and the ribbon-like g-C_3N_4. The inset in (a) is the Tauc plot providing the band gaps. The optical images of the samples are also shown as insets in both figures, with solar light irradiation in (a) and 365 nm UV irradiation in (b).

It has been reported that different solvents could lead to different assemblies.[48] We tried to obtain precipitates from the dispersion by adding different alcohols, including methanol, ethanol, n-propanol and isopropanol. Various special assemblies could be obtained accordingly, as shown in Fig. 4, and Table S1. Belts can be formed by adding methanol, ethanol and n-propanol (Fig. 4a). In addition, beautiful flower clusters are generated by adding ethanol or n-propanol (Fig. 4b-f). It can be observed that the flower clusters are composed of many ribbons. These ribbons stretch out from the plinth and scatter outward, like a bouquet of blooming flowers. Upon adding isopropanol, rods and tubes become the overwhelming morphologies (Fig.4g-i).

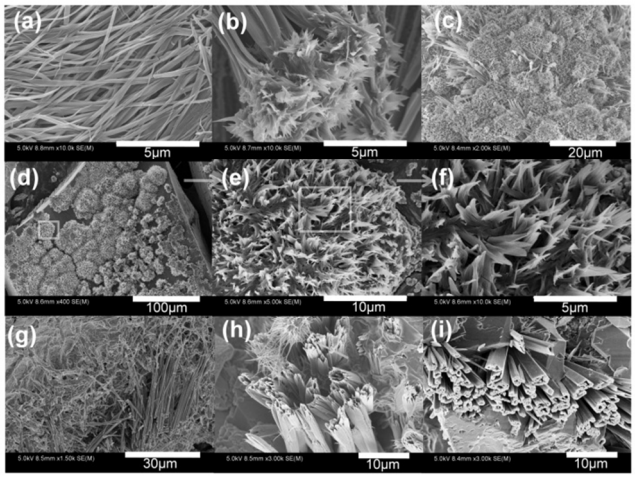

Figure 4. Microstructures of the special assemblies: (a) belts, (b-f) flower clusters, (g) rods, and (h-i) tubes.

Energy dispersion analysis (EDS) was performed on the assemblies to analyze the distribution of elements, as shown in Fig. S5-6. We could observe that in most areas the elements are in accordance with the XPS full scan analysis shown in Fig. S1, that is, the atomic fractions of C, N, O, Na, Cl are in the range of 35~46, 44~50, 1~8, 7~12, 0~4 at%, respectively. Some crystal-like areas could also be observed belonging to NaCl.

Based on the above results, it can be concluded that grinded NaCl acts a very good small template for the polymerization of DCDA and modifies the chemical and microstructures of g-C_3N_4. A possible mechanism is proposed in Sch. 1 and Fig. S7. DCDA and NaCl were finely mixed on grinding, and many fresh surfaces of NaCl crystals were formed. Due to the electronegativity of these surfaces, strong interaction was formed between NaCl and amino of DCDA. Melon, which is linear, was generated by the polymerization of DCDA (Fig. S8).[44] Upon further cross-linking, melon generates ribbon-like g-C_3N_4 sheets.[49] Because of the catalytic effect of NaCl, the triazine units of g-C_3N_4 adsorbed on NaCl may decompose generating cyano groups, observed in quantity above 550℃ (Fig. S3-4).

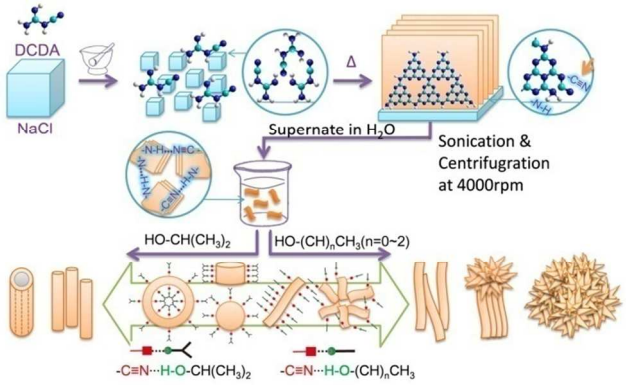

Scheme 1. Schematic diagram of the formation of ribbon-like g-C_3N_4 and various assemblies (for clarity, sizes are not represented proportionally).

The formation mechanism of the special assemblies is also illustrated in Sch. 1. After adding alcohols, the hydrogen bond forms between cyano group of ribbon-like g-C_3N_4 and hydroxyl of alcohol, so that the dispersion of the ribbon-like g-C_3N_4 becomes unstable and begins to precipitate. g-C_3N_4 stacks together forming long and thin belts. Different alcohols have different structures and steric hindrances, leading to different microstructures of assemblies. Methanol, ethanol and n-propanol are linear and their steric hindrance is relatively low. So belts are formed (Fig. 4a). However, compared with methanol, ethanol and n-propanol exhibit relatively higher steric hindrance, which make the ribbons tend to arrange in loose bundles. The ends of the bundles are easy to bloom outward due to the repulsive interaction between the alkyl ends of the alcohols, which generates beautiful flower clusters (Fig. 4b-f). Isoparopanol, with a Y-shaped molecular structure, exhibits much higher steric hindrance, which makes the ribbons tend to generate rigid rods (Fig. 4g) and tubes (Fig. 4h-i).

Conclusions

In summary, ribbon-like g-C_3N_4 was generated on the fresh surface of NaCl. Cyano group was regenerated due to the catalytic effect of NaCl. These microstructures, as well as the slight content of Na^+ ions, give g-C_3N_4 the enhanced optical performance and exceptional dispersion in water. Based on the hydrogen bonding and steric hindrance, various special assemblies can be obtained. This work presents a novel green and simple way to make ribbons and assemblies of g-C_3N_4, offering them many new potential applications.

Acknowledgements

The project was supported by Hunan Provincial Natural Science Foundation for Distinguished Young Scholars (14JJ1001) and National Natural Science Foundation of China (51073172).

Notes and references

College of Science, National University of Defense Technology, Changsha 410073, P. R. China. Fax:86-731-84574250; Tel: 86-731-84574786-811; E-mail: chuzy@nudt.edu.cn

† Electronic Supplementary Information (ESI) available: Experimental, XPS, SEM, EDS, FTIR, TG and reaction illustrations. See DOI: 10.1039/b000000x/

1 Zhang J. S.; Wang B.; Wang X. C. *Prog. Chem.* **2014**, *26* , 19.
2 Dong G. P.; Zhang Y.H.; Pan Q.W.; Qiu J. R. *J. Photoch. Photobio. C.*; **2014**, *20*, 33.
3 Wang, X.; Blechert, S.; Antonietti, M. *ACS Catal.* **2012,** *2* , 1596.
4 Wang Y., Wang X.C. Antonietti M. *Angew. Chem. Int. Ed.* **2012,** *51*, 68.
5 Cao, S. W.; Yu, J.G. *J. Phys. Chem. Lett.* **2014**, *5*, 2101.
6 Chu, Z.Y.; Yuan, B.; Yan, T.N. *J. Inorg. Mater.* **2014**, 29, 785.
7 Bai, X.; Wang, L.; Zong, R.; Zhu, Y. *J. Phys. Chem. C* **2013,** *117*, 9952.
8 Liao, G.; Chen, S.; Quan, X.; Yu, H.; Zhao, H. *J. Mater. Chem.* **2012,** *22* , 2721.
9 Yang, S.; Gong, Y.; Zhang, J.; Zhan, L.; Ma, L.; Fang, Z.; Vajtai, R.; Wang, X.; Ajayan, P. M. *Adv. Mater.* **2013,** *25*, 2452.
10 Su, F.; Mathew, S. C.; Möhlmann, L.; Antonietti, M.; Wang, X.; Blechert, S. *Angew. Chem. Int. Ed.* **2011,** *50*, 657.
11 Tian, J.; Ning, R.; Liu, Q.; Asiri, A. M.; Al-Youbi, A. O.; Sun, X. *ACS Appl. Mater. Interfaces* **2013,** *6*, 1011.
12 Chen, L.; Huang, D.; Ren, S.; Dong, T.; Chi, Y.; Chen, G. *Nanoscale* **2013,** *5*, 225.
13 Tian, J.; Liu, Q.; Asiri, A. M.; Al-Youbi, A. O.; Sun, X. *Anal. Chem.* **2013,** *85*, 5595.
14 Xu, H.; Yan, J.; She, X.; Xu, L.; Xia, J.; Xu, Y.; Song, Y.; Huang, L.; Li, H. *Nanoscale* **2014,** *6*, 1406.
15 Zhang, S.; Li, J.; Zeng, M.; Xu, J.; Wang, X. K.; Hu, W. *Nanoscale* **2014**, *6*, 4157.
16 Cheng, C.; Huang, Y.; Wang, J.; Zheng, B.; Yuan, H.; Xiao, D. *Anal. Chem.* **2013,** *85*, 2601.
17 Zhang, Y.; Antonietti, M. *J. Am. Chem. Soc.* **2010,** *132*, 6294.
18 Zhang, Y.; Antonietti, M. *Chem. Asian* **2010,** *5* , 1307.
19 Bu, Y.; Chen, Z.; Yu, J.; Li, W. *Electrochim. Electrochim. Acta.* **2013,** *88*, 294.
20 Zhang, X.; Xie, X.; Wang, H.; Zhang, J.; Pan, B.; Xie, Y. *J. Am. Chem. Soc.* **2013,** *135*, 18.
21 Lin, L. S.; Cong, Z. X.; Li, J.; Ke, K. M.; Guo, S. S.; Yang, H. H.; Chen, G. N. *J. Mater. Chem. B* **2014,** *2*, 1031.
22 Wu, M.; Wang, Q.; Sun, Q.; Jena, P. *J. Phys. Chem. C* **2013,** *117*, 6055.
23 Zhu, G.; Lü, K.; Sun, Q.; Kawazoe, Y.; Jena, P. *Comput. Mater. Sci.* **2014,** *81*, 275.
24 Hou, Y.; Wen, Z.; Cui, S.; Guo, X.; Chen, J. *Adv. Mater.* **2013,** *25* , 1.
25 Li, X. H.; Chen, J. S.; Wang, X.; Sun, J.; Antonietti, M. *J. Am. Chem. Soc.* **2011,** *133*, 8074.

26 Wang, Y.; Zhang, J.; Wang, X.; Antonietti, M.; Li, H. *Angew. Chem. Int. Ed.* 2010**,** *49*, 3356.
27 Cheng, N.; Tian, J.; Liu, Q.; Ge, C.; Qusti, A. H.; Asiri, A. M.; Al-Youbi, A. O.; Sun, X. *ACS Appl. Mater. Interfaces* **2013,** *5*, 6815.
28 Dong, G.; Zhang, L. *J. Mater. Chem.* **2012,** *22*, 1160.
29 Chu, S.; Wang, Y.; Guo, Y.; Feng, J.; Wang, C.; Luo, W.; Fan, X.; Zou, Z. *ACS Catal.* **2013,** *3* , 912.
30 Liang, C. D.; Hong, K. L.; Guiochon, G. A.; Mays, J. W.; Dai, S. *Angew. Chem. Int. Ed.* **2004**, 43, 5785.
31 Liang C. D.; Li, Z. J.; Dai, S. *Angew. Chem. Int. Ed*. **2008**, 47, 3696.
32 Zhang, J.S.; Zhang, M.W.; Sun, R. Q.; Wang, X.C. *Angew. Chem. Int. Ed.* **2012**, 51, 10145.
33 Xu, J.; Wang, Y.; Zhu, Y. *Langmuir* **2013,** *29*, 10566.
34 Liu, G.; Niu, P.; Sun, C. H.; Smith, S. C.; Chem, Z. G.; Lu, G. Q.; Cheng, H. M. *J. Am. Chem. Soc.* **2010**, 132, 11642.
35 Cui, Y.J.; Ding, Z.X.; Fu, X.Z.; Wang, X.C. *Angew. Chem. Int. Ed.* **2012**, 51, 11814.
36 Lin, Z.Z.; Wang, X.C. *Angew. Chem. Int. Ed.* **2013**, 52, 1735.
37 Wirnhier, E.; Doblinger M.; Gunzelmann D.; Senker J.; Lotsch, B.V.; Schnick W. *Chem. Eur.* **2011,** 17, 3213.
38 Niu, P.; Zhang, L.; Liu, G.; Cheng, H. M. *Adv. Funct. Mater.* **2012,** *22*, 4763.
39 Tian, J.Q.; Liu, Q.; Asiri, A.M.; Qusti, A.H.; Al-Youbi, A.O.; Sun, X.P. *Nanoscale* **2013**, 5, 11604.
40 Tian, J.Q.; Liu, Q.; Ge, C.J.; Xing, Z.C.; Asiri, A.M.; Al-Youbi, A.O.; Sun, X.P. *Nanoscale* **2013**, 5, 8921.
41 Tian, J.Q.; Liu, Q.; Asiri, A.M.; Alamry, K.A.; Sun, X.P. *ChemSusChem* **2014**, DOI: 10.1002/cssc.201402118.
42 Li, X. H.; Zhang, J.; Chen, X.; Fischer, A.; Thomas, A.; Antonietti, M.; Wang, X. *Chem. Mater.* **2011,** *23*, 4344.
43 Li, X.-H.; Wang, X.; Antonietti, M. *ACS Catal.* **2012,** *2*, 2082.
44 Wang, X.; Maeda, K.; Thomas, A.; Takanabe, K.; Xin, G.; Carlsson, J. M.; Domen, K.; Antonietti, M. *Nat Mater* **2009,** *8*, 76.
45 Li, J.; Shen, B.; Hong, Z.; Lin, B.; Gao, B.; Chen, Y. *Chem. Commun.* **2012,** *48*, 12017.
46 Tahir, M.; Cao, C.; Mahmood, N.; Butt, F. K.; Mahmood, A.; Idrees, F.; Hussain, S.; Tanveer, M.; Ali, Z.; Aslam, I. *ACS Appl. Mater. Interfaces* **2013,** *6*, 1258.
47 Ge, L.; Zuo, F.; Liu, J.; Ma, Q.; Wang, C.; Sun, D.; Bartels, L.; Feng, P. *J. Phys. Chem. C* **2012,** *116*, 13708.
48 Dong, R.; Bo, Y.; Tong, G.; Zhou, Y.; Zhu, X.; Lu, Y. *Nanoscale* **2014**, *6*, 4544.
49 Tyborski, T.; Merschjann, C.; Orthmann, S.; Yang, F.; Lux-Steiner, M. C.; Schedel-Niedrig, Th. *J. Phys.: Condens. Matter* **2013,** *25*, 395402.

